

First principles study of heavy oil organonitrogen adsorption on NiMoS hydrotreating catalysts

Mingyong Sun^a, Alan E. Nelson^{a,*}, John Adjaye^b

^a University of Alberta, Department of Chemical and Materials Engineering, Edmonton, Alta., Canada T6G2G6

^b Syncrude Canada Ltd., Edmonton Research Centre, Edmonton, Alta., Canada T6N1H4

Available online 3 October 2005

Abstract

The adsorption of quinoline, acridine, indole, and carbazole on the well-defined NiMoS hydrotreating catalyst edge surface has been studied by means of density-functional theory (DFT) using a periodic supercell model. Quinoline and acridine, the basic nitrogen-containing molecules present in heavy oils, are preferably adsorbed on the Ni-edge surface through the lone pair electrons of the nitrogen atom, which produces relatively high adsorption energies ($-\Delta E_a = 16\text{--}26 \text{ kcal mol}^{-1}$). Indole and carbazole, the non-basic nitrogen-containing molecules, primarily interact with the NiMoS catalyst edge surface through the π -electrons of the carbon atoms. While indole preferentially adsorbs on the NiMoS surface through the β -carbon of the pyrrolic ring ($-\Delta E_a = 19 \text{ kcal mol}^{-1}$), carbazole primarily interacts with the NiMoS surface through the phenyl rings ($-\Delta E_a = 13 \text{ kcal mol}^{-1}$). The relative adsorptivities and energetically preferred adsorption modes of the nitrogen-containing molecules in heavy oils can provide insights into experimental observations about hydrodenitrogenation (HDN) kinetics and reaction pathways.

© 2005 Elsevier B.V. All rights reserved.

Keywords: Adsorption; NiMoS; Hydrodenitrogenation; Quinoline; Indole; Acridine carbazole; Heavy oil; Density-functional theory

1. Introduction

The increasing demand for processing heavy oils and vacuum residue, which contain significantly more nitrogen compounds than conventional light crude oils, requires the development of hydrotreating catalysts with higher hydrodenitrogenation (HDN) activity. In order to develop new hydrotreating catalysts with high activity to remove refractory nitrogen compounds present in heavy oils, a detailed understanding of HDN catalysis, including the structure of the catalysts, the electronic configurations of the nitrogen compounds, and the adsorption and reaction mechanisms of basic and non-basic nitrogen compounds on catalyst surfaces, is required.

Molybdenum-based sulfides are widely used in the oil refining industry as hydrotreating catalysts to remove sulfur and nitrogen from heavy oils. The active phase on these hydrotreating catalysts has a MoS₂-like structure, and active sites are located at edge surfaces of the MoS₂ [1,2]. Due to extensive experimental and theoretical research, a good

understanding of the structure of the active phase at the atomic level and the location of promoters (nickel and cobalt) in the active phase has been achieved. For unpromoted MoS₂, the ($\bar{1}010$) S-edge and ($10\bar{1}0$) Mo-edge are normally covered by bridge sulfur atoms and have very few sulfur vacancies at reaction conditions [3–5]. In the promoted catalysts, cobalt prefers to incorporate into the S-edge and nickel to the Mo-edge of MoS₂, and the promoted edge surfaces have more vacant sites under typical hydrotreating reaction conditions [6–8].

Most nitrogen present in heavy crude oils is in the form of heterocyclic organonitrogen compounds containing basic (pyridinic) or non-basic (pyrrolic) ring structures [9]. Non-basic nitrogen compounds are a significant fraction of the total nitrogen content in heavy oils [10,11]. These non-basic nitrogen compounds are more difficult to remove than basic nitrogen compounds using conventional NiMoS catalysts. Indeed, it has been shown that a narrow boiling fraction of coker gas oil containing more non-basic carbazoles and tetrahydrocarbazoles was more inhibitory and deactivated the catalyst to a greater degree in the HDN of quinoline [12]. This difference in reactivity has largely been attributed to the weaker adsorptivity of non-basic nitrogen compounds compared to basic nitrogen compounds [13,14]. Basic and non-basic

* Corresponding author. Tel.: +1 780 492 7380; fax: +1 780 492 2881.

E-mail address: alan.nelson@ualberta.ca (A.E. Nelson).

nitrogen compounds have distinct electronic structures and properties that determine their differences in adsorption energetics and reaction pathways on catalyst surfaces [15]. Unfortunately, detailed information regarding the adsorption of organonitrogen compounds on hydrotreating catalyst surfaces has not been reported, specifically for larger organonitrogen molecules in heavy oils containing two or three rings.

There are several studies about the adsorption of sulfur-containing molecules on the unpromoted MoS_2 surface, including thiophene [16,17], benzothiophene [18], and dibenzothiophene [19,20], which have provided some insights into hydrodesulfurization (HDS) reaction mechanisms. However, no similar work has been done for nitrogen-containing compounds, particularly on the industrially relevant nickel-promoted MoS_2 catalyst (NiMoS). Previous studies have been reported for the adsorption of pyridine on a hydrogenated MoS_2 surface by the CNDO/UHF method [21], and we recently investigated the adsorption of pyridine and pyrrole on a NiMoS catalyst [22]. In the context of hydroprocessing heavy oils, higher molecular weight organonitrogen molecules such as quinoline, indole, acridine, and carbazole become significant. Therefore, the objective of the present study is to investigate the adsorption of high molecular weight organonitrogen molecules on the active nickel-promoted NiMoS edge surface [4,7,8].

2. Experimental methods

The catalyst model used in the present study is shown in Fig. 1, which has also been used in our previous study [22]. The model is repeated in the x -direction with a periodicity of six MoS_2 units, and separated by vacuum layers of 15 Å in the y - and z -directions. The volume of the supercell is 19.0 Å \times 24.6 Å \times 18.4 Å. On the edge surface of this representation are nickel atoms that substitute surface molybdenum atoms. In the very large

supercell, the interaction between the organonitrogen molecules and the catalyst surface will not be affected by molecules in the neighbouring cells.

The calculations are based on density-functional theory (DFT), and have been performed using Material Studio DMol³ from Accelrys[®] (Version 2.2) [23]. The DNP basis sets and GGA-PW91 exchange-correlation functionals are used in all calculations [24,25]. The real space cutoff radius is 4.5 Å. All electron basis sets are used for light elements, such as hydrogen, oxygen, and sulfur. Effective Core Potentials [26,27] are used to treat core electrons of molybdenum and nickel, and a k -point of (1 \times 1 \times 1) was used because of the large supercell. Spin polarization was applied to all calculations.

3. Results and discussion

In nickel-promoted molybdenum sulfide catalysts, nickel atoms prefer to incorporate into the MoS_2 structure by substituting molybdenum atoms at the (10 $\bar{1}$ 0) Mo-edge of MoS_2 [8], thus generating a so-called Ni-edge surface as shown in Fig. 1. In the following discussions, the adsorption of organonitrogen molecules was studied using a Ni-edge surface including six nickel atoms in a supercell; however, only a part of the nickel layer is shown in subsequent figures to summarize the different adsorption modes. The adsorption energies (ΔE_a) are calculated as the differences in electronic energies between the adsorption complex and clean surface plus gas-phase molecule. The negative ΔE_a values indicate that adsorption is an exothermic process.

3.1. Adsorption of basic nitrogen-containing compounds

Quinoline can be adsorbed on the Ni-edge of NiMoS with the molecular plane parallel to the Ni-edge plane via side-on adsorption, or with the molecular plane perpendicular to the Ni-edge plane as end-on adsorption. Several possible adsorption modes were studied for both side-on and end-on configurations. The side-on configurations resulted in very weak interactions as evidenced by small adsorption energies ($-\Delta E_a < 5 \text{ kcal mol}^{-1}$); thus, it can be concluded that no strong interaction exists between quinoline and NiMoS through side-on adsorption.

Table 1 summarizes the most stable configurations of quinoline on the Ni-edge in which quinoline is perpendicular or tilted to the Ni-edge surface bonding through N–Ni interaction. The end-on configurations with the nitrogen atom bonding to a nickel site through a N–Ni bond (Structures 1a and 1b) result in large adsorption energies ($-\Delta E_a > 21 \text{ kcal mol}^{-1}$). The repulsion effect between the hydrogen atoms of the phenyl ring and the Ni-edge surface results in a smaller adsorption energy when quinoline is orientated along the Ni-edge plane (Structure 1a, $-\Delta E_a = 21.2 \text{ kcal mol}^{-1}$) than when the phenyl moiety is away from the catalyst plane (Structure 1b, $-\Delta E_a = 26.3 \text{ kcal mol}^{-1}$). However, the presence of neighbouring slabs would interact with the out-of-plane phenyl ring, thus, affecting the stability of Structure 1b. Although Structure 1a would not be affected by the presence of neighbouring MoS_2

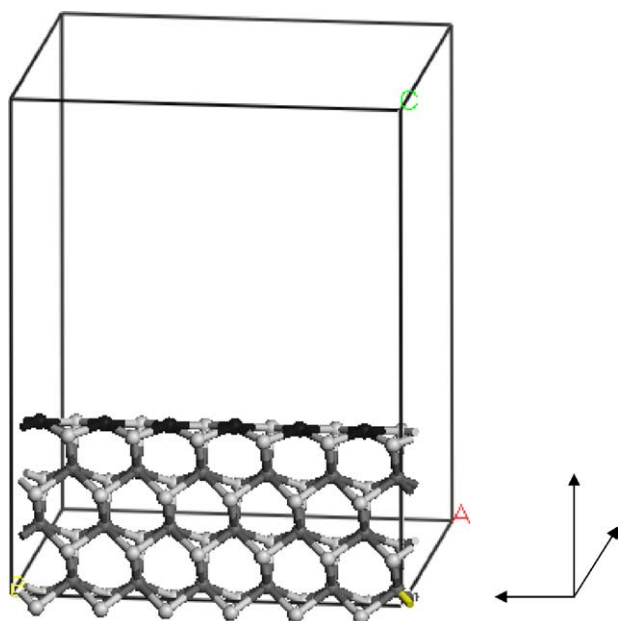


Fig. 1. Catalyst model: black—nickel, dark grey—molybdenum, light grey—sulfur.

Table 1

Surface configurations of quinoline (1a and 1b) and acridine (1c and 1d) on the Ni-edge surface after optimization and the relative energies of optimized configurations with the clean surface and gas-phase molecule as energetic references

Configurations	Optimized geometry	$-\Delta E_a$ (kcal mol $^{-1}$)
1a		21.2
1b		26.3
1c		15.9
1d		18.9

slabs, Structure 1b can only be considered for the adsorption of quinoline on the top layer edge surface for a multilayer MoS₂ structure with the phenyl ring protruding above the catalyst surface. The most important result from these studies is that quinoline tends to be adsorbed on the Ni-edge surface with the end-on configuration through Ni–N bonding. This would (partly) explain why the hydrogenation of the nitrogen-containing ring is faster than that of the phenyl ring [28], even though the phenyl ring has higher π -electron density [15].

The adsorption of acridine on the Ni-edge surface with both side-on and end-on adsorption configurations was also studied. For side-on adsorption of acridine, the two phenyl rings deform out of the aromatic plane towards the NiMoS surface and the centre nitrogen ring moves away from the surface. This configuration only generates a small adsorption energy, $-\Delta E_a = 7.6$ kcal mol $^{-1}$; thus, similar to the adsorption of quinoline, acridine is unlikely to adsorb on the Ni-edge surface via side-on adsorption. Acridine positioned on the surface with the nitrogen atom directly atop of a nickel site with the two phenyl rings oriented along the edge plane (Structure 1c) bonds to the NiMoS edge with an adsorption energy of $-\Delta E_a = 15.9$ kcal mol $^{-1}$. Acridine cannot adsorb on the NiMoS edge surface along the edge plane, as quinoline does (Structure

1a), due to the hindrance of the hydrogen atoms on the phenyl rings (Structure 1c). However, if there are a sufficient number of vacant edge nickel sites, acridine can adsorb on the NiMoS edge in a slightly tilted configuration (Structure 1c). While Structure 1d yields a larger adsorption energy ($-\Delta E_a = 18.9$ kcal mol $^{-1}$), the presence of neighbouring slabs would strongly decrease the adsorption energy, and possibly preclude this adsorption mode, as has been shown for dibenzothiophene on unpromoted MoS₂ [20].

3.2. Adsorption of non-basic nitrogen-containing compounds

End-on adsorption through N–Ni bonding is not possible for non-basic nitrogen-containing molecules due to the electronic structure of the pyrrolic ring [15]. For side-on adsorption, the most stable configuration for indole is through the C₃–Ni bonding as shown in Table 2 (Structure 2a). The adsorption energy for this adsorption mode is $-\Delta E_a = 18.7$ kcal mol $^{-1}$. This adsorption mode activates the pyrrolic ring, which results in the hydrogenation of the nitrogen ring prior to the phenyl ring [29,30].

During the parallel adsorption of carbazole on NiMoS, the centre pyrrolic ring is repulsed away from the NiMoS edge surface while the two phenyl rings are attracted towards the surface (Structure 2b). This mode of carbazole adsorption yields an adsorption energy of $-\Delta E_a = 12.5$ kcal mol $^{-1}$. From this configuration, it is apparent that the interaction between the phenyl rings and the edge surface is stronger than the interaction between the nitrogen ring and the surface. In order to confirm this observation, carbazole was rotated 90° relative to the NiMoS edge plane and either a phenyl ring or the centre pyrrolic ring was positioned above the edge plane. The configuration with the phenyl ring above the surface produces a larger adsorption

Table 2

Surface configurations of indole (2a) and carbazole (2b and 2c) on the Ni-edge surface after optimization and the relative energies of optimized configurations with the clean surface and gas-phase molecule as energetic references

Configurations	Optimized geometry	$-\Delta E_a$ (kcal mol $^{-1}$)
2a		18.7
2b		12.5
2c		13.1

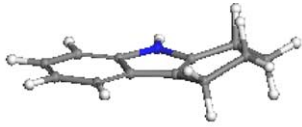
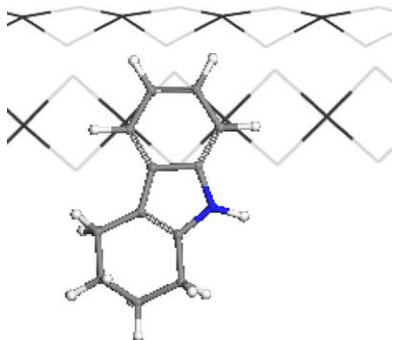
energy (Structure 2c, $-\Delta E_a = 13.1 \text{ kcal mol}^{-1}$) than the configuration with the pyrrolic ring above the surface (configuration not shown, $-\Delta E_a = 8.3 \text{ kcal mol}^{-1}$). These results clearly indicate that carbazole prefers to interact with the Ni-edge surface through the phenyl ring(s), as opposed to the pyrrolic ring, which is contrast to indole.

In addition to carbazole, tetrahydrocarbazole also contributes a significant portion to the nitrogen content of heavy oil, and consequently is of concern in the hydroprocessing of heavy oil [12]. Table 3 shows the adsorption configurations of tetrahydrocarbazole on the Ni-edge with the three rings orientated along or across the edge plane. After the saturation of one phenyl ring, tetrahydrocarbazole prefers to interact with the NiMoS surface through the unsaturated phenyl ring. This indicates that the pyrrolic ring will not significantly interact with the catalyst surface until the phenyl rings are completely saturated. Thus, the removal of the nitrogen atom from carbazole and tetrahydrocarbazoles is difficult during conventional hydrotreating processes.

3.3. Implications to hydrodenitrogenation

In catalytic HDN, it is generally accepted that nitrogen-containing molecules are adsorbed on the NiMoS surface prior to reaction, and thus, the adsorptivities of the nitrogen-containing molecules affects their relative reactivities [31,32]. The adsorption configuration of the basic and non-basic nitrogen molecules on the catalyst surface also affects the reaction pathways [22]. Quinoline and acridine are adsorbed on the edge surface through a strong interaction between the nitrogen atom and a nickel site, which makes the nitrogen ring more readily to be hydrogenated. This is consistent with experimental observations that indicate the saturation of the nitrogen ring is always faster than that of the phenyl ring in the HDN of quinoline and acridine [12,13,28,33].

Table 3
Surface configurations of tetrahydrocarbazole on the Ni-edge surface after optimization and the relative energies of optimized configurations with the clean surface and gas-phase molecule as energetic references

Configurations	Optimized geometry	$-\Delta E_a$ (kcal mol $^{-1}$)
3a		12.2
3b		13.6

For non-basic nitrogen compounds, indole is preferably adsorbed on the catalyst edge surface via the C₃ carbon atom on the nitrogen ring (Structure 2a), while carbazole bonds to the NiMoS edge surface through the phenyl ring (Structures 2b and 2c). It is interesting to note that the difference in the preferred hydrogenation moiety between indole and carbazole corresponds very well to the differences in their adsorption modes. The hydrogenation of a phenyl ring is the first step in the HDN of carbazole [34,35] while the hydrogenation of the nitrogen ring is favoured over that of the phenyl ring in the HDN of indole [29,30].

For the HDN of a mixture of basic and non-basic compounds, the basic nitrogen compounds always show a higher reactivity than their non-basic analogs [13,36]. In the simultaneous HDS and HDN processes, the basic nitrogen compounds normally show a stronger inhibition effect than non-basic nitrogen compounds towards HDS reactions [35,36]. These experimental observations can, at least partly, be explained by the theoretical results of this study, which indicate that all basic nitrogen compounds have higher adsorption energy than non-basic nitrogen compounds. The energetics and the geometries of different nitrogen compounds on catalyst surfaces provide a fundamental basis for further studies on HDN reaction mechanisms and for the development of new catalysts with higher HDN activity and selectivity.

4. Conclusions

The adsorption of quinoline and acridine on the Ni-edge surface of NiMoS occurs primarily through Ni–N bonding. The presence of the additional phenyl ring in acridine decreases the adsorption energy compared to quinoline. The adsorption of indole on the Ni-edge preferably takes place via C₃–Ni interaction. Carbazole, with an additional phenyl ring compared to indole, preferably interacts with the catalyst surface with the phenyl ring. Tetrahydrocarbazole is likely adsorbed on the Ni-edge surface through the phenyl ring with a similar adsorption energy as carbazole. Generally, basic nitrogen-containing compounds have higher adsorption energy than non-basic nitrogen compounds, which results in their higher HDN reactivities and stronger inhibition effects in HDN and HDS reactions. A good correlation exists between the preferred reaction pathways and the most stable adsorption geometries of these nitrogen-containing molecules; the preferred adsorbed moiety is always hydrogenated preferably in HDN processes.

Acknowledgements

This work is supported by Syncrude Canada Ltd. and the Natural Sciences and Engineering Research Council (NSERC) under Grant No. CRDPJ 261129.

References

- [1] R. Prins, V.H.J. de Beer, G.A. Somorjai, Catal. Rev. Sci. Eng. 31 (1989) 1.
- [2] H. Topsøe, B.S. Clausen, F.E. Massoth, Hydrotreating Catalysis, Science and Technology, vol. 11, Springer Verlag, Berlin, 1996.

- [3] L.S. Byskov, J.K. Nørskov, B.S. Clausen, H. Topsøe, *J. Catal.* 187 (1999) 109.
- [4] P. Raybaud, J. Hafner, G. Kresse, S. Kasztelan, H. Toulhoat, *J. Catal.* 189 (2000) 129.
- [5] M. Sun, J. Adjaye, A.E. Nelson, *Appl. Catal. A: Gen.* 263 (2004) 131.
- [6] J.V. Lauritsen, S. Helveg, E. Lægsgaard, I. Stensgaard, B.S. Clausen, H. Topsøe, F. Besenbacher, *J. Catal.* 197 (2001) 1.
- [7] H. Schweiger, P. Raybaud, H. Toulhoat, *J. Catal.* 212 (2002) 33.
- [8] M. Sun, A.E. Nelson, J. Adjaye, *J. Catal.* 226 (2004) 32.
- [9] J.F. Cocchetto, C.N. Satterfield, *Ind. Eng. Chem. Process. Des. Dev.* 15 (1976) 272.
- [10] G.C. Laredo, S. Leyva, R. Alvarez, M.T. Mares, J. Castillo, J.L. Cano, *Fuel* 81 (2002) 1341.
- [11] M. Dorbon, C. Bernasconi, *Fuel* 68 (1989) 1068–1074.
- [12] W. Kanda, I. Siu, J. Adjaye, A.E. Nelson, M.R. Gray, *Energy Fuels* 18 (2004) 539.
- [13] D. Ferdous, A.K. Dalai, J. Adjaye, *Energy Fuels* 17 (2003) 164.
- [14] S. Shin, K. Sakanishi, I. Mochida, *Energy Fuels* 14 (2000) 539.
- [15] M. Sun, A.E. Nelson, J. Adjaye, *J. Mol. Catal. A: Chem.* 222 (2004) 243.
- [16] P. Raybaud, G. Kresse, J. Hafner, H. Toulhoat, *Phys. Rev. Lett.* 80 (1998) 1481.
- [17] H. Orita, K. Uchida, N. Itoh, *J. Mol. Catal. A* 193 (2003) 197.
- [18] S. Cristol, J.-F. Paul, E. Payen, D. Bougeard, F. Hutschka, J. Hafner, *Stud. Surf. Sci. Catal.* 128 (1999) 327.
- [19] H. Yang, C. Fairbridge, Z. Ring, *Energy Fuels* 17 (2003) 387.
- [20] S. Cristol, J.-F. Paul, E. Payen, D. Bougeard, F. Hutschka, S. Clémendot, *J. Catal.* 224 (2004) 138.
- [21] E.N. Rodríguez-Arias, A.E. Gainza, A.J. Hernández, P.S. Lobos, F. Ruetter, *J. Mol. Catal. A: Chem.* 102 (1995) 163.
- [22] M. Sun, A.E. Nelson, J. Adjaye, *J. Catal.* 231 (2005) 223.
- [23] B. Delley, *J. Chem. Phys.* 113 (2000) 7756.
- [24] A.D.J. Becke, *Chem. Phys.* 88 (1988) 2547.
- [25] J.P. Perdew, Y. Wang, *Phys. Rev. B* 45 (1992) 13244.
- [26] M. Dolg, U. Wedig, H. Stoll, H. Preuss, *J. Chem. Phys.* 86 (1987) 866.
- [27] A. Bergner, M. Dolg, W. Kuechle, H. Stoll, H. Preuss, *Mol. Phys.* 80 (1993) 1431.
- [28] C.N. Satterfield, S.H. Yang, *Ind. Eng. Chem. Process. Des. Dev.* 23 (1984) 13.
- [29] E.O. Odeunmi, D.F. Ollis, *J. Catal.* 80 (1983) 87.
- [30] L. Zhang, U.S. Ozkan, *Stud. Surf. Sci. Catal.* 101 (1996) 1223.
- [31] G. Perot, *Catal. Today* 10 (1991) 447.
- [32] R. Prins, *Adv. Catal.* 46 (2001) 399.
- [33] M.J. Girgis, B.C. Gates, *Ind. Eng. Chem. Res.* 30 (1991) 2038.
- [34] M. Nagai, Y. Goto, A. Irisawa, S. Omi, *J. Catal.* 191 (2000) 128.
- [35] G.C. Laredo, A. Montesinos, J.A. De los Reyes, *Appl. Catal. A: Gen.* 265 (2004) 171.
- [36] T. Koltai, M. Macaud, A. Guevara, E. Sculz, M. Lemaire, R. Baccud, M. Vrinat, *Appl. Catal. A: Gen.* 231 (2002) 253.